Mon. Not. R. Astron. Soc. **000**, 000–000 (0000) Printed 17 September 2014 (MN LaTeX style file v2.2)

CoMaLit III. Literature Catalogs of weak Lensing Clusters of galaxies (LC^2)

Mauro Sereno[1]*
[1]*Dipartimento di Fisica e Astronomia, Università di Bologna, viale Berti Pichat 6/2, 40127 Bologna, Italia*

17 September 2014

ABSTRACT
The measurement of the mass of clusters of galaxies is crucial for their use in cosmology and astrophysics. Masses can be efficiently determined with weak lensing (WL) analyses. I compiled from Literature a Catalog of weak Lensing Clusters (LC^2). Cluster identifiers, coordinates, and redshifts have been standardised. WL masses were reported to over-densities of 2500, 500, 200, and to the virial one in the reference ΛCDM model. Duplicate entries were carefully handled. I produced three catalogs: LC^2-*single*, with 485 unique groups and clusters analysed with the single-halo model; LC^2-*substructure*, listing substructures in complex systems; LC^2–*all*, listing all the 822 WL masses found in literature. The catalogs are publicly available at https://www.dropbox.com/sh/hukhb24c3ahiun2/AADVuW7yUAA2XjyDrFwofejAa?dl=0

Key words: galaxies: clusters: general – gravitational lensing: weak – catalogues

1 INTRODUCTION

Clusters of galaxies are at the crossroad between cosmology and astrophysics. They are laboratories to study the physics of the baryons and of the dark matter at large scales in bound objects (Voit 2005; Pratt et al. 2009; Arnaud et al. 2010; Giodini et al. 2013). Cosmological parameters can be measured with cluster abundances and the observed growth of massive galaxy clusters (Mantz et al. 2010; Planck Collaboration et al. 2013), with gas fractions (Ettori et al. 2009) or lensing analyses (Sereno 2002; Jullo et al. 2010; Lubini et al. 2013). This requires precise and accurate measurements of the cluster masses.

Cluster properties that can be easily measured with ongoing and future large surveys (Laureijs et al. 2011), such as optical richness, X-ray luminosity, Sunyaev-Zel'dovich (SZ) flux, ..., are going to be used as mass proxies. This relies on an accurate calibration through comparison with direct mass estimates (Andreon & Bergé 2012; Ettori 2013; Sereno & Ettori 2014; Sereno, Ettori & Moscardini 2014).

Weak lensing (WL) analyses provide one of the most well regarded mass estimate. The physics behind gravitational lensing is well understood. The shear distortions of the background galaxies trace the gravitational field of the matter distribution of the lens (Hoekstra et al. 2012; von der Linden et al. 2014; Umetsu et al. 2014).

Even if the WL estimate of the total projected mass along the line of sight is precise, the approximations that have to be used (spherical symmetry, smooth density distributions, no other contribution along the line of sight, ...) to infer the three-dimensional mass may bias and scatter the results.

The main sources of uncertainty in WL mass estimates are due to triaxiality and substructures. The spherical assumption can bias the results for triaxial clusters pointing towards the observer, wherein lensing strengths are boosted and mass and concentration are over-estimated, or for clusters elongated in the plane of the sky, as happens for most of the halos in a randomly selected sample, wherein mass and concentration are on the contrary under-estimated (Oguri et al. 2005; Sereno 2007; Corless, King & Clowe 2009; Sereno, Jetzer & Lubini 2010; Sereno & Umetsu 2011; Sereno & Zitrin 2012).

Substructures in the cluster surroundings dilute the tangential shear signal (Meneghetti et al. 2010; Giocoli et al. 2012, 2014). Significant mass under-estimations are caused by either massive sub-clumps (Meneghetti et al. 2010) or uncorrelated large-scale matter projections along the line of sight (Becker & Kravtsov 2011).

Numerical studies have quantified the extent to which bias and intrinsic scatter affect WL masses. Usual fitting procedures of the cluster tangential shear profiles can bias low the mass by ∼5–10 per cent with a scatter of ∼10–25 per cent (Meneghetti et al. 2010; Becker & Kravtsov 2011; Rasia et al. 2012). The scatter should be less significant in optimally selected clusters either having regular morphology or living in substructure-poor environments (Rasia et al. 2012).

These theoretical predictions agree with recent measurements. Sereno & Ettori (2014) recently determined an intrinsic scatter for WL masses of ∼15 per cent.

An alternative and popular method to infer the cluster mass is based on the assumption that hydrostatic equilibrium holds be-

* E-mail: mauro.sereno@unibo.it (MS)

tween the intra-cluster medium (ICM) and the gravitational potential. The cluster mass can then be recovered from observations of the spatially resolved spectroscopic data and the X-ray surface brightness (LaRoque et al. 2006; Donahue et al. 2014). However, deviations from equilibrium or non-thermal contributions to the pressure are difficult to quantify and can bias the mass estimate to a larger extent than for WL masses (Rasia et al. 2012; Sereno & Ettori 2014).

Other methods to derive the cluster mass employ spectroscopic measurements of galaxies velocities, such as the caustic technique (Rines & Diaferio 2006) or approaches exploiting the Jeans equation (Lemze et al. 2009; Biviano et al. 2013). These methods are hindered by the very expensive observational requirements and are mostly limited to low redshift halos.

Since WL masses can be obtained up to high redshifts, they require observational programs feasible in the context of large surveys, and they are nearly unbiased, they are supposedly the best mass estimators to calibrate other proxies.

In this paper I re-elaborate in a standard form known WL mass estimates of galaxy clusters available in literature. The typical information presented in WL studies is not standardised. A cluster can be named in different ways. Different conventions are employed for the reference cosmological model. The lens can be characterised in a number of ways. A quantitative analysis can provide either the total mass within an integration radius (which on turn can be defined in several ways), or the total projected mass within an angular aperture (this is the quantity the lensing is most sensitive to), or the parameters characterising the adopted mass profile.

I collected all the disparate WL measurements available in literature in three meta-catalogs regularised to the same reference cosmology and to the same set of integration radii. The basic characteristics of these catalogues are the large number of objects (485 unique systems), and the standardised names, coordinates, redshifts and masses. References to the original analyses were reported for each cluster.

I compiled three catalogues: i) the LC^2-*single* lists the unique systems. Duplicate entries originating from overlaps between the input references were controlled and eliminated. The reported masses of either regular or complex clusters were obtained with a single-halo analysis. These are the most sensible masses to compare to other global properties, such as the SZ flux, the X-ray luminosity or the optical richness. ii) The LC^2-*substructure* lists the main and the secondary substructures of complex clusters which were studied with a multiple-halo analysis. The mass of each component is reported individually. iii) The LC^2-*all* lists all the groups and clusters found in literature. Repeated entries are included. LC^2-*single* and LC^2-*substructure* are subsamples of LC^2-*all*.

The catalogs are publicly available in electronic format and will be periodically updated.

For the compilation of the catalogs, I assumed a fiducial flat ΛCDM cosmology with density parameter $\Omega_{\rm M0} = 0.3$, and Hubble constant $H_0 = 70\ {\rm km\ s^{-1} Mpc^{-1}}$. When H_0 is not specified, h is the Hubble constant in units of $100\ {\rm km\ s^{-1} Mpc^{-1}}$.

This paper is the third in a series titled 'CoMaLit' (COmparing MAsses in LITerature). In the first paper (Sereno & Ettori 2014), systematic differences in lensing and X-ray masses obtained from independent analyses were quantified and the overall level of bias and intrinsic scatter was assessed through Bayesian techniques. This formalism was later applied to calibrate the Sunyaev-Zel'dovich (SZ) flux estimated by the Planck satellite against mass proxies (Sereno, Ettori & Moscardini 2014).

The papers is structured as follows. In Section 2, I comment on qualities and drawbacks of meta-catalogues collected from literature and their use in astronomy. In Section 3, I review the various definitions of over-density and virial radii and I motivate the choice of the radii used for the catalogs. In Section 4, I review the most used mass density distributions to characterise the lens and I discuss how I standardised the estimates of the masses listed in the catalogs. Section 5 discusses the dependence of the WL mass estimates on the cosmological parameters and how they can be uniformed to a given reference cosmological model. In Section 6, I discuss how I assembled the catalogs from the various literature sources and how I performed the cluster identifications. Section 7 is devoted to the presentation of the format of the catalogs. Final consideration are in Section 8.

2 ON META-CATALOGUES

The worthiness of coherently compiled meta-catalogues of clusters has been discussed in Piffaretti et al. (2011), who collected a large catalogue of X-ray detected clusters of galaxies based on publicly available samples.

Specifically to the WL catalogs here presented, I remark that the LC^2-*all* provides a panorama of the state-of-the-art on weak lensing clusters. It gives an overview of the published, publicly available weak lensing analyses. It is a repository of references and a ready-to use collection of the main properties (coordinates, redshift and mass) of the observed clusters.

Large, standardised catalogues can be used for cross-correlation with existing, ongoing or upcoming surveys in various wave-lengths, such as SZ (Planck Collaboration et al. 2013; Reichardt et al. 2013; Menanteau et al. 2013), optical (Laureijs et al. 2011, Euclid), or X-ray surveys (Piffaretti et al. 2011, and references therein). The mass, in combination with the appropriate scaling laws, enables us to predict all the main properties of the clusters, such as the integrated SZ flux, the X-ray temperature, the optical richness, and the velocity dispersion.

The largest public catalogs of massive WL clusters consists of a few dozens of objects (Shan et al. 2012; Mahdavi et al. 2013; Applegate et al. 2014; Umetsu et al. 2014). Clusters are not usually selected according to strict selection functions and some sort of arbitrariness can persist. The usual WL sample that can be found in literature is then small but it is neither statistical nor complete. It can be worthy to take a different route, i.e., to consider a sample whose selection function is not known but that is as large as possible. A very large sample, no matter whether it was assembled in a heterogeneous way, can recover the actual physical trends we are looking for (Gott et al. 2001).

The LC^2 catalogues can be useful for the construction of better defined subsamples. The full sample of collected clusters is neither statistical nor complete. The reconstruction of the selection function of meta-catalogues is a nearly impossible task (Piffaretti et al. 2011). The individual selection functions of the subsamples are complex and, in most cases, are not known or not available. However, suitable subsamples can be extracted for which the selection function can be approximated. These subsamples can be used to study scaling relations, time evolution of structures, and cosmography.

A large collection of clusters enables us to assess the reliability of the WL mass measurements (Sereno & Ettori 2014). The repeated entries in LC^2-*all* can be used to compare mass estimates from different analyses. Published uncertainties are often unable to account for the actual variance seen in sample pairs (Rozo et al.

2014; Sereno & Ettori 2014). The certain assessment of cluster masses is hindered by instrumental and methodological sources of errors which may cause systematic uncertainties in data analysis (Rozo et al. 2014). The main sources of systematics in lensing analyses are due to selection and calibration problems. The selection and redshift measurement of background galaxies is a very difficult task that has to be undertaken through accurate photometric redshifts and colour-colour selection methods (Medezinski et al. 2010; Gruen et al. 2014). A small calibration correction of the shear signal of the order of just a few percents can produce a systematic error of $\sim$ 10 per cent in the estimate of the virial mass (Umetsu et al. 2014). Differences in WL mass estimates reported by different groups can be as large as $\sim$40 per cent (Sereno & Ettori 2014).

Even though the catalogues are presented in a uniform format, I remark that they are highly heterogeneous. The clusters were detected in a variety of ways within X-ray, optical, SZ or shear surveys. Some clusters were targeted because they are very peculiar objects, as merging (Okabe & Umetsu 2008) or high-redshift clusters (Jee et al. 2011). Some samples of clusters were assembled based on their known properties, as their X-ray luminousity or regular X-ray morphology (Mahdavi et al. 2013; von der Linden et al. 2014; Umetsu et al. 2014). Others were observed in follow-up programs of differently planned surveys, which significantly increased the number of studied lensing clusters and extended the observation range to lower mass objects (Kettula et al. 2013; McInnes et al. 2009). Some samples were shear selected (Shan et al. 2012).

On the positive end, systematic biases that affect some specific, small samples may average out in a heterogeneous and very large sample. The larger the sample, the smaller the biases due to the orientation of the clusters, to their internal structure, and to the projection effect of large-scale structure. Due to the different finding techniques, biases plaguing lensing selected samples, such as the over-concentration problem and the orientation bias (Oguri & Blandford 2009; Meneghetti et al. 2011), are mitigated too. Projection effects are less severe in X-ray or SZ detected clusters.

The different observational facilities and data analysis methods also increase the heterogeneous nature of the catalog. Different solutions to instrumental and methodological sources of errors may cause systematic errors in the mass determination. The heterogeneity of the catalogs manifests both in the listed central estimates and the uncertainties. Masses are presented in a homogeneous way but they were not derived homogeneously among the original studies.

3 MASSES

Total masses of clusters within an over-dense region can be related to the virial mass. Most cluster properties are expected to be self-similar at those scales. There are several commonly used definitions of the virial radius. Over-densities can be measured either with respect to the critical density of the universe at the epoch of analysis, (Δ_c) or with respect to the mean density (Δ_m). For the compilation of the catalog, I took $\Delta = \Delta_c$, in terms of which important properties of galaxy clusters are universal (Diemer & Kravtsov 2014).

M_Δ denotes the mass within the radius r_Δ, which encloses a mean over-density of Δ times the critical density at the cluster redshift, $\rho_\mathrm{cr} = 3H(z)^2/(8\pi G)$; $H(z)$ is the redshift dependent Hubble parameter. By definition, M_Δ can be expressed as

$$M_\Delta = \frac{4\pi}{3}\Delta\rho_\mathrm{cr} r_\Delta^3. \quad (1)$$

Numerical simulations showed that fixed over-densities are very useful to describe universal features of clusters and to study the scaling relations (Tinker et al. 2008; Diemer & Kravtsov 2014). From the theoretical point of view, the virialized region of a cluster can be related to the solution to the collapse of top-hat perturbations. The viral over-density is then redshift and cosmology dependent. To compute the virial radius, I adopted the approximated relation proposed by Bryan & Norman (1998) and based on the spherical collapse model for a flat universe with cosmological constant,

$$\Delta_\mathrm{vir} \simeq 18\pi^2 + 82[\Omega_\mathrm{M}(z) - 1] - 39[\Omega_\mathrm{M}(z) - 1]^2. \quad (2)$$

WL studies probe the clusters on large radial scales. As integration radii, I considered the virial radius and r_{200}, which usually enclose most of the field of view covered by observations and are also well probed by SZ analyses; r_{500}, which still encloses a substantial fraction of the total virialised mass of the system and is usually the largest radius probed in X-ray observations; r_{2500}, which is usually poorly constrained by WL alone, but that can still be useful in comparison with detailed analysis of the cluster core, as those based on current high resolution X-ray observations or strong lensing investigations. Results at r_{2500} are mostly based on extrapolations and they may be unreliable without strong lensing constraints.

The critical surface density for lensing is defined as

$$\Sigma_\mathrm{cr} \equiv \frac{c^2\, D_\mathrm{s}}{4\pi G\, D_\mathrm{d}\, D_\mathrm{ds}}, \quad (3)$$

where D_s, D_d and D_ds are the source, the lens and the lens-source angular diameter distances, respectively.

4 MASS PROFILES

Whenever the masses M_Δ were quoted in the original papers, I took them for the catalogs. If not, I had to extrapolate the quoted results based on the density profile adopted in the analysis. The Navarro-Frenk-White profile (Navarro, Frenk & White 1996, NFW), and the singular isothermal sphere (SIS) are the standard parametric models used in lensing analyses to characterise the deflector.

Alternatively, some works quote only the total projected mass in an angular aperture. This may be the case of combined strong and weak lensing analyses or of free-form modelling. In this cases, I extrapolated the results by adopting a NFW model.

4.1 NFW

Dark matter halos are successfully described as NFW density profiles (Navarro, Frenk & White 1996; Jing & Suto 2002). The 3D density distribution follows

$$\rho_\mathrm{NFW} = \frac{\rho_\mathrm{s}}{(r/r_\mathrm{s})(1+r/r_\mathrm{s})^2}, \quad (4)$$

where r_s is the scale radius. The mass enclosed at radius r is

$$M_\mathrm{NFW}(<r) = 4\pi\ \rho_\mathrm{s}\ r_\mathrm{s}^3 F_\mathrm{NFW}(r_\mathrm{s}/r), \quad (5)$$

where

$$F_\mathrm{NFW}(x) = x^3\left[\ln(1+x^{-1}) - (1+x)^{-1}\right]. \quad (6)$$

The NFW model is characterized by two parameters. They can be ρ_s and r_s or the mass M_Δ and the concentration, $c_\Delta \equiv r_\Delta/r_\mathrm{s}$. The conversion relations are simple. From the definition of concentration and Eq. (5),

$$r_\mathrm{s} = r_\Delta/c_\Delta \quad (7)$$

and

$$\rho_{\rm s} = \frac{\Delta}{3}\frac{1}{F_{\rm NFW}(1/c_\Delta)}\rho_{\rm cr}. \quad (8)$$

The general conversion from a mass at an arbitrary over-density, Δ_1, to a second one, Δ_2, was derived in Hu & Kravtsov (2003). By writing the parameters $r_{\rm s}$ and $\rho_{\rm s}$ in terms of two different over-densities through Eqs. (7 and 8) and equating the expressions, we obtain

$$F_{\rm NFW}\left(\frac{1}{c_{\Delta_2}}\right) = \frac{\Delta_2}{\Delta_1}F_{\rm NFW}\left(\frac{1}{c_{\Delta_1}}\right), \quad (9)$$

$$M_{\Delta_2} = \frac{\Delta_2}{\Delta_1}\left(\frac{c_{\Delta_2}}{c_{\Delta_1}}\right)^3 M_{\Delta_1}. \quad (10)$$

The conversion involves the inversion of the function $F_{\rm NFW}(x)$.

Equations (9, 10) can also be rewritten to derive the concentrations given two integrated masses, M_{Δ_1} and M_{Δ_2},

$$F_{\rm NFW}\left(\frac{1}{c_{\Delta_1}}\left(\frac{\Delta_2 M_{\Delta_1}}{\Delta_1 M_{\Delta_2}}\right)^{1/3}\right) = \frac{\Delta_2}{\Delta_1}F_{\rm NFW}\left(\frac{1}{c_{\Delta_1}}\right); \quad (11)$$

given two masses and one concentration, the remaining concentration can be obtained as

$$c_{\Delta_2} = c_{\Delta_1}\left(\frac{\Delta_1 M_{\Delta_2}}{\Delta_2 M_{\Delta_1}}\right)^{1/3}. \quad (12)$$

An additional relation has to be used to constrain the profile if only one parameter is known. N-body simulations have proved that mass and concentration are related (Neto et al. 2007; Gao et al. 2008; Duffy et al. 2008; Prada et al. 2012; Dutton & Macciò 2014; Diemer & Kravtsov 2014). In limited ranges, the dependence of the halo concentration on mass and redshift can be adequately described by a power law,

$$c_{200} = A(M_{200}/M_{\rm pivot})^B(1+z)^C. \quad (13)$$

If only one parameter is reported in the analysis, I broke the degeneracy in the mass profile by adopting the relation in Eq. (13) with $A = 5.71 \pm 0.12$, $B = -0.084 \pm 0.006$, and $C = -0.47 \pm 0.04$ for a pivotal mass $M_{\rm pivot} = 2\times10^{12}M_\odot/h$ (Duffy et al. 2008).

Some analyses quote only the projected mass within an aperture radius. The total projected mass for a NFW lens can be expressed as

$$M^{\rm cyl}_{\rm NFW}(<R) = 4\pi\rho_{\rm s}r_{\rm s}^3\left\{2\frac{\text{arctanhh}\left|\frac{1-x}{1+x}\right|}{\sqrt{|1-x^2|}} + \ln\left(\frac{x}{2}\right)\right\}, \quad (14)$$

where x is the dimensionless projected radius, $x \equiv R/r_{\rm s}$, and arctanhh = arctanh (arctan) if $x < (>)1$. If only the mass within a cylinder, $M^{\rm cyl}_{\rm obs}$, is provided, the mass M_Δ can be derived by inverting

$$M^{\rm cyl}_{\rm NFW}(R_{\rm obs}; M_\Delta, c_\Delta(M_\Delta)) = M^{\rm cyl}_{\rm obs}, \quad (15)$$

where $c_\Delta(M_\Delta)$ can be expressed as in Eq. (13).

4.2 Singular Isothermal sphere

An alternative mass profile is provided by the singular isothermal sphere, whose density profile is

$$\rho_{\rm SIS} = \frac{1}{2\pi}\frac{\sigma^2_{\rm SIS}}{G}\frac{1}{r^2}. \quad (16)$$

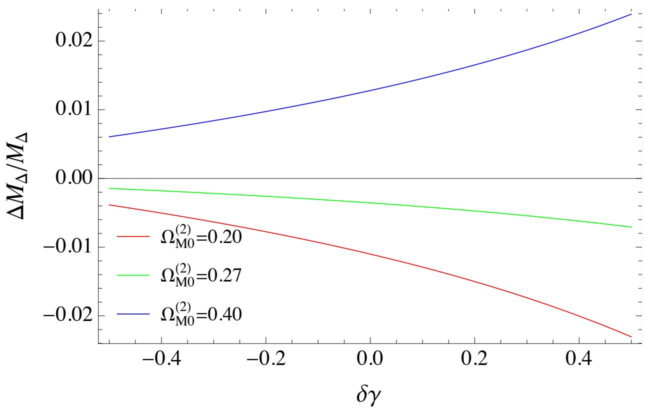

Figure 1. Relative variation of the estimated WL mass within a fixed over-density, M_Δ, as a function of the slope $\delta\gamma$ for different (flat) cosmological models with respect to the standard ΛCDM model with $\Omega_{\rm M0} = 0.3$. The lens redshift is $z_{\rm d} = 0.3$; the background galaxies are at $z_{\rm s} = 1.0$. The red, green, and blue lines refer to flat ΛCDM models with $\Omega_{\rm M0}$ =0.20, 0.27 and 0.40, respectively

This model was the standard for lens profiles before being supplanted by the NFW model. The total mass within a spherical radius is

$$M_{\rm SIS}(<r) = \frac{2\sigma^2_{\rm SIS}}{G}r. \quad (17)$$

It follows that

$$r_\Delta = \frac{2\sigma^2_{\rm SIS}}{H(z)\sqrt{\Delta}}, \quad (18)$$

and

$$M_\Delta = \frac{4\sigma^3_{\rm SIS}}{GH(z)\sqrt{\Delta}}. \quad (19)$$

5 COSMOLOGICAL PARAMETERS

Lensing mass estimates depend on the assumed cosmological model. If necessary, they were rescaled to the reference cosmological model, i.e., a flat ΛCDM cosmology with density parameter $\Omega_{\rm M0} = 0.3$, and Hubble constant $H_0 = 70\ {\rm km\,s^{-1}Mpc^{-1}}$.

The conversion from other cosmological models was detailed in Sereno & Ettori (2014). The lensing 3D mass within a radius $r = D_{\rm d}\theta$, where θ is the angular radius, scales as

$$M^{\rm WL} \propto \Sigma_{\rm cr}D_{\rm d}^2\theta_{\rm E}\,\theta f(\theta), \quad (20)$$

where $\theta_{\rm E}$ is the angular Einstein radius. The function $f(\theta) \sim \theta^{\delta\gamma}$ quantifies the deviation of the mass profile from the isothermal case.

By equating Eq. (1) and Eq. (20) at $\theta_\Delta (= r_\Delta/D_{\rm d})$, we obtain

$$M^{\rm WL}_\Delta \propto D_{\rm d}^{-\frac{3\delta\gamma}{2-\delta\gamma}}\left(\frac{D_{\rm ds}}{D_{\rm s}}\right)^{-\frac{3}{2-\delta\gamma}}H(z)^{-\frac{1+\delta\gamma}{1-\delta\gamma/2}}. \quad (21)$$

Equation (21) holds for a fixed over-density, whereas the viral over-density depends on the cosmological parameters. For the virial mass,

$$M^{\rm WL}_{\rm vir} \propto \Delta_{\rm vir}^{-\frac{1+\delta\gamma}{2-\delta\gamma}}D_{\rm d}^{-\frac{3\delta\gamma}{2-\delta\gamma}}\left(\frac{D_{\rm ds}}{D_{\rm s}}\right)^{-\frac{3}{2-\delta\gamma}}H(z)^{-\frac{1+\delta\gamma}{1-\delta\gamma/2}}, \quad (22)$$

where $\Delta_{\rm vir}$ is a function of the redshift dependent cosmological density, $\Omega_{\rm M}$.

The dependence on the cosmological parameters is usually small. The variation is $\lesssim 2$ per cent for a large range of mass profiles and cosmological models, see Fig. 1.

The condition $\delta\gamma = 0$ is strictly verified only for the singular isothermal profile but it provides a good approximation in general. Let us consider as a typical massive lens, a NFW distribution with $M_{200} \simeq 10^{15} M_\odot$ and $c_{200} \simeq 3$. The deviation of the slope from the isothermal value is small over a large radial range, with $\delta\gamma(r_{2500}) \simeq 0.4$, $\delta\gamma(r_{500}) \simeq 0.0$, $\delta\gamma(r_{200}) \simeq -0.1$, $\delta\gamma(r_{\rm vir}) \simeq -0.2$.

To make the proper conversion from different cosmological parameters, I used by default $\delta\gamma = 0$, when Eq. (21) reduces to

$$M_\Delta^{\rm WL} \propto \left(\frac{D_{\rm ds}}{D_{\rm s}}\right)^{-3/2} H(z)^{-1}. \quad (23)$$

and Eq. (22) can be simplified as

$$M_{\rm vir}^{\rm WL} \propto \Delta_{\rm vir}(\Omega_{\rm M})^{-\frac{1}{2}} \left(\frac{D_{\rm ds}}{D_{\rm s}}\right)^{-3/2} H(z)^{-1}. \quad (24)$$

6 CATALOG COMPILATION

I included in the catalog all groups and clusters with weak lensing analyses I was aware of. The research in literature was performed thanks to the NASA's Astrophysics Data System[1]. A public list of clusters with weak lensing analyses, compiled by H. Dahle and last updated in 2007, was also used[2].

The compilation of the first version of the catalogs was based on 69 weak lensing studies comprising 822 analyses of individual groups and clusters, see Table 1.

The catalogs were meant to avoid re-elaboration as much as possible. Masses quoted in the reference papers were directly reported. When original estimates were provided with asymmetric errors, I computed the mean value and the standard deviation as suggested in D'Agostini (2004). Missing masses were computed by extrapolation as discussed in Sec. 4. Corrections for the cosmological model were performed as detailed in Sec. 5.

Masses were redetermined with a fitting procedure in three cases. The fitting procedure is detailed in Sereno et al. (2014). Briefly, the observed shear profile is fitted to a spherical NFW functional through the function,

$$\chi^2_{\rm WL}(M_{200}, c_{200}) = \sum_i \left[\frac{g_+(\theta_i) - g_+^{\rm NFW}(\theta_i; M_{200}, c_{200})}{\delta_+(\theta_i)}\right]^2, \quad (25)$$

where g_+ is the reduced tangential shear at angular position θ (Wright & Brainerd 2000) and δ_+ is the observational uncertainty.

When a strong lensing constraint was available, the effective angular Einstein radius $\theta_{\rm E}$ was fitted through

$$\chi^2_{\rm SL}(M_{200}, c_{200}) = \left[\frac{\theta_{\rm E} - \theta_{\rm E}^{\rm NFW}(M_{200}, c_{200})}{\delta\theta_{\rm E}}\right]^2. \quad (26)$$

The total likelihood is $\mathcal{L} \propto \exp\{-(\chi^2_{\rm WL} + \chi^2_{\rm SL})/2\}$. For the catalog, I considered uniform priors in the ranges $0.02 \leqslant M_{200}/(10^{14} h^{-1} M_\odot) \leqslant 100$ and $0.02 \leqslant c_{200} \leqslant 20$. The parameters and their uncertainties were finally derived as the bi-weight estimators of the marginalised posterior probability densities.

For the Local Cluster Substructure Survey (LOCUSS) sample

[1] http://www.adsabs.harvard.edu/
[2] http://folk.uio.no/hdahle/WLclusters.html

Table 1. Number of clusters, groups or substructures ($N_{\rm clusters}$ in col. 3), analysed in each reference, col. 1. The authors' code is listed in col. 2.

Reference		$N_{\rm clusters}$
Shan et al. (2012)	shan+12	87
Hoekstra et al. (2012)	hoekstra+12	55
Applegate et al. (2014)	applegate+14	51
Mahdavi et al. (2013)	mahdavi+13	50
Dahle et al. (2002)	dahle+02	38
McInnes et al. (2009)	mcinnes+09	36
Dahle (2006)	dahle06	35
Sereno & Covone (2013)	sereno&13	31
Okabe et al. (2010)	okabe+10	30
Pedersen & Dahle (2007)	pedersen&07	30
Oguri et al. (2012)	oguri+12	28
Hamana et al. (2009)	hamana+09	27
Jee et al. (2011)	jee+11	27
Hoekstra et al. (2011)	hoekstra+11	25
Cypriano et al. (2004)	cypriano+04	24
Clowe et al. (2006)	clowe+06	20
Umetsu et al. (2014)	umetsu+14	20
Merten et al. (2014)	merten+14	19
Gruen et al. (2014)	gruen+14	12
Limousin et al. (2009)	limousin+09	12
Bardeau et al. (2007)	bardeau+07	11
Foëx et al. (2012)	foex+12	11
Kettula et al. (2013)	kettula+13	10
Smail et al. (1997)	smail+97	10
Abate et al. (2009)	abate+09	9
Okabe & Umetsu (2008)	okabe&08	9
Gavazzi & Soucail (2007)	gavazzi&07	8
Israel et al. (2012)	israel+12	8
Kubo et al. (2009)	kubo+09	7
Watanabe et al. (2011)	watanabe+11	6
Clowe et al. (2000)	clowe+00	6
High et al. (2012)	high+12	5
Umetsu et al. (2011)	umetsu+11	5
Okabe et al. (2011)	okabe+11	4
Umetsu et al. (2009)	umetsu+09	4
Melchior et al. (2014)	melchior+14	4
Okabe et al. (2014b)	okabe+14b	4
Corless, King & Clowe (2009)	corless+09	3
Gray et al. (2002)	gray+02	3
Gavazzi et al. (2004)	gavazzi+04	3
Jee et al. (2014)	jee+14	3
Bradač et al. (2006)	bradac+06	2
Hamilton-Morris et al. (2012)	hamilton-morris+12	2
Dietrich et al. (2009)	dietrich+09	2
Bradač et al. (2008a)	bradac+08b	2
Bradač et al. (2008b)	bradac+08a	1
Clowe, Gonzalez & Markevitch (2004)	clowe+04	1
Gavazzi (2005)	gavazzi05	1
Gavazzi et al. (2009)	gavazzi+09	1
Halkola, Seitz & Pannella (2006)	halkola+06	1
Hicks et al. (2007)	hicks+07	1
Huang et al. (2011)	huang+11	1
Jauzac et al. (2012)	jauzac+12	1
Jauzac et al. (2014)	jauzac+14	1
Kubo et al. (2007)	kubo+07	1
Lerchster et al. (2011)	lerchster+11	1
Limousin et al. (2007)	limousin+07	1
Limousin et al. (2010)	limousin+10	1
Mahdavi et al. (2007)	mahdavi+07	1
Margoniner et al. (2005)	margoniner+05	1
Merten et al. (2011)	merten+11	1
Miyatake et al. (2013)	miyatake+13	1
Oguri et al. (2013)	oguri+13	1
Okabe et al. (2014a)	okabe+14a	1
Paulin-Henriksson et al. (2007)	paulin-henriksson+07	1
Radovich et al. (2008)	radovich+08	1
Romano et al. (2010)	romano+10	1
Schirmer et al. (2010)	schirmer+10	1
Schirmer et al. (2011)	schirmer+11	1

in Okabe et al. (2010), I fitted the published shear profiles in order to derive the masses of all the 30 clusters of the sample, rather than the 26 reported in Okabe et al. (2010, table 6). Shear measurements in Okabe et al. (2010) are biased low due to contamination effects and systematics in shape measurements (Okabe et al. 2013). We then corrected the fitted masses according to the factors reported in Okabe et al. (2013, table 2).

I also refitted the clusters previously analysed in Sereno & Covone (2013). The fitting procedure was slightly improved since, see (Sereno et al. 2014). For the catalog, I then used the updated mass determinations.

Finally, Mahdavi et al. (2007) published the shear profile of ABELL 478 but they did not report the mass determination. Values listed in the catalogs are the result of the fitting I performed.

6.1 Intentional omissions

There was a number of intentional omissions. I required that each lensing cluster was confirmed by independent observations. Lensing peaks without an optical, X-ray or SZ counterpart were excised from the catalog. This may be the case of some weak-lensing shear-selected halos or lensing peaks found in pilot programs targeting fields centred on active galactic nuclei or quasars (Wold et al. 2002).

I did not include some lensing analyses of single clusters that were later refined/improved by the same authors or collaboration. Just as an example, this is the case of the analyses of the high redshift clusters in Jee et al. (2005a,b), Jee et al. (2006), and Jee & Tyson (2009) that were later revised in Jee et al. (2011).

I considered only lensing studies performed under the assumption of spherical symmetry. Unfortunately, there is just a handful of clusters with triaxial analyses (Oguri et al. 2005; Corless, King & Clowe 2009; Sereno & Umetsu 2011; Sereno et al. 2013; Morandi et al. 2012; Limousin et al. 2013, and references therein). For homogeneity reasons, I excluded them.

Complex cluster morphologies may be separated in multiple peaks by high resolution WL analyses. To compile the catalog with unique entries, LC^2-*single*, I only considered masses measured with a single halo analysis. Masses of substructures and multiple peaks associated to the same clusters are reported in the LC^2-*substructure* catalog.

6.2 Cluster identifications

The same cluster may appear in several analyses under different names and with different quoted redshifts and locations. To standardise the notation, I reported the NASA/IPAC Extragalactic Database[3] (NED) preferred name and the NED's coordinates and redshift for each object. Most of the clusters were identified by name. A few of them were associated by matching positions.

Since most of the lenses which were not associated by name in NED are secondary halos in merging or complex systems, or shear-selected peaks found in dense fields, I could not adopt a fixed search radius when cross-checking with the NED. In fact, a blind matching based on a fixed aperture can associate the same NED counterpart to multiple, separate lenses, which we know to be distinct according to the reference paper. The association by position was then performed cluster-by-cluster. A limited number of lenses, mostly SZ or shear-selected halos, lacked the NED identification.

Control of repeated entries was performed by looking for repeated NED associations. For clusters which were not identified by querying the NED, I also looked for matches of both position and redshift. If the cluster's coordinates were missing in the original papers, I used the location obtained from querying the NED.

7 CATALOG PRESENTATION

I compiled three catalogs. The LC^2-*single* lists all clusters and groups whose mass was determined with a single-halo modelling, no matter what the dynamical state, and contains virtually no multiple entries.

The LC^2-*substructure* lists separately the main components and the secondary haloes of complex systems, whose masses were derived with a multiple-halo analysis. As for LC^2-*single*, duplicate entries were eliminated. There is some redundancy between LC^2-*single* and LC^2-*substructure*. Some systems may appear as a single halo in LC^2-*single* and as a main halo with substructures in LC^2-*substructure*.

LC^2-*all* comprises the full body of information I found and reduced from literature. Multiple entries are present, as well as single- or multiple-halo analyses of the same lens. The LC^2-*single* and LC^2-*substructure* are subsamples with unique entries of LC^2-*all*. When a cluster had multiple analyses available in literature, I picked for the LC^2-*single* either the most recent analysis or that based on deeper observations.

Table 2 presents an extract of LC^2-*single*, in terms of the first 50 entries. In each catalog, objects are ordered by right ascension. The format is as follows.

Cols. 1-2: name of cluster as designated in the original lensing paper.

Cols. 3-4: right ascension RA (J2000) and declination DE (J2000), as quoted in the original lensing paper. If coordinates are not quoted in the source paper or in a companion one, I reported the coordinates of the NED's association.

Col. 5: redshift z, as reported in the original lensing paper.

Col. 6: external validation through NED. 'N': the NED's object was associated by name; 'P': the NED's object was associated by positional matching; 'NA': no found association.

Cols. 7-11: as in cols. 1-5, but for the NED's association.

Col. 12: author code.

Col. 13: ADS's bibliographic code.

Cols. 14-15: over-density mass M_{2500} and related uncertainty δM_{2500}, in units of $10^{14} M_\odot$.

Cols. 16-17: as for cols. 14-15, but for the over-density mass M_{500}.

Cols. 18-19: as for cols. 14-15, but for the over-density mass M_{200}.

Cols. 20-21: as for cols. 14-15, but for the virial mass M_{vir}.

7.1 Basic properties

I discuss the basic properties of the collected clusters. 507 clusters, groups, or sub-structures were analysed in published lensing studies. 131 objects were studied by at least two independent groups. The most popular targets are ABELL 209, 1835, and 2261, with ten independent analyses each, and ABELL 611 and 1689 (9 analyses each). Overall, we found 822 mass determinations.

The *single* catalog contains 485 unique entries. The redshift distribution of the (unique) clusters (see Fig. 2) has a large range,

[3] http://ned.ipac.caltech.edu/

Table 2. The first 50 entries of the LC^2-single catalogue. The full catalogs are available in electronic form. Columns are described in Section 8.

Name (1-2)	Right Ascension (J2000) (3)	Declination (J2000) (4)	z (5)	Match (6)	NED's primary name (7-8)	NED's RA (J2000) (9)	NED's DE (J2000) 10)	NED's z (11)	Autor Code (12)	ADS's bibcode (13)	M_{2500} $[10^{14}M_\odot]$ (14)	δM_{2500} $[10^{14}M_\odot]$ (15)	M_{500} $[10^{14}M_\odot]$ (16)	δM_{500} $[10^{14}M_\odot]$ (17)	M_{200} $[10^{14}M_\odot]$ (18)	δM_{200} $[10^{14}M_\odot]$ (19)	$M_{\rm vir}$ $[10^{14}M_\odot]$ (20)	$\delta M_{\rm vir}$ $[10^{14}M_\odot]$ (21)
ABELL 2744	00:14:20.67	–30:24:00.86	0.308	N	ABELL 2744	00:14:18.90	–30:23:22.0	0.308	merten+11	2011MNRAS.417..333M	4.962	1.597	15.412	4.959	24.054	7.741	29.025	9.340
CL 0016+16	00:18:33.445	+16:26:13.00	0.547	N	Cl 0016+16	00:18:33.84	+16:26:16.6	0.541	applegate+14	2014MNRAS.439...48A	7.122	1.842	17.821	4.609	25.756	6.661	29.101	7.526
ABELL 22	00:20:38.6	–25:43:19.2	0.141	N	ABELL 22	00:20:42.80	–25:42:37.0	0.142352	cypriano+04	2004ApJ...613...95C	1.012	0.512	2.263	1.146	3.578	1.812	4.760	2.410
ACT-CL J0022.2-0036	00:22:13.0	–00:36:33.8	0.805	NA	NA NA	NA	NA	NA	miyatake+13	2013MNRAS.429.3627M	2.824	1.456	7.860	4.053	11.798	6.083	13.118	6.764
MACS J0025.4-1222	00:25:29.907	–12:22:44.64	0.585	N	MACS J0025.4-1222	00:25:29.38	–12:22:37.1	0.5843	applegate+14	2014MNRAS.439...48A	3.965	1.392	9.922	3.483	14.340	5.034	16.130	5.663
Cl 0024+17	00:26:36.0	+17:08:36	0.39	N	ZwCl 0024.0+1652	00:26:35.70	+17:09:46.0	0.39	umetsu+11	2011ApJ...729..127U	6.600	0.900	12.329	1.943	17.057	2.686	18.986	3.200
CL 0030+2618	00:30:33.6	+26:18:16	0.5	N	WARP J0030.5+2618	00:30:33.20	+26:18:19.0	0.5	israel+12	2012A%26A...546A..79I	1.803	0.516	4.512	1.292	6.521	1.867	7.412	2.122
ABELL 68	00:37:05.947	+09:09:36.02	0.255	N	ABELL 68	00:37:05.30	+09:09:11.0	0.255	applegate+14	2014MNRAS.439...48A	3.665	0.634	9.171	1.587	13.254	2.294	15.670	2.712
ABELL 85	00:41:48.7	–09:19:04.8	0.056	N	ABELL 85	00:41:50.10	–09:18:07.0	0.055061	cypriano+04	2004ApJ...613...95C	2.048	0.557	4.579	1.245	7.240	1.968	9.947	2.704
ABELL 2811	00:42:07.9	–28:32:09.6	0.108	N	ABELL 2811	00:42:08.70	–28:32:09.0	0.107908	cypriano+04	2004ApJ...613...95C	1.767	0.849	3.952	1.898	6.248	3.000	8.414	4.040
ABELL 115	00:55:59.8	+26:22:40.8	0.1971	N	ABELL 115	00:55:59.80	+26:22:41.0	0.1971	okabe+10	2010PASJ...62..811O	1.478	0.936	4.832	3.061	7.427	4.705	9.108	5.771
Cl 0054-27	00:56:37.4	–27:30:47	0.56	N	ABELL 2843	00:56:37.38	–27:30:46.7	0.56	smail+97	1997ApJ...479...70S	1.131	0.619	3.391	1.857	5.227	2.862	6.012	3.292
RX J0056.9-2740	00:56:56.98	–27:40:29.9	0.563	N	Cl 0054-2756	00:56:56.87	–27:40:30.1	0.56	hoekstra+11	2011ApJ...726...48H	0.640	0.360	1.862	1.048	2.840	1.597	3.255	1.831
ACT-CL J0102-4915	01:02:52.50	–49:14:58.0	0.87	N	SPT-CL J0102-4915	01:02:53.00	–49:15:19.0	0.75	jee+14	2014ApJ...785...20J	4.391	0.847	16.800	3.200	25.400	4.900	28.661	5.529
ABELL 141	01:05:36.3	–24:39:20	0.23	N	ABELL 141	01:05:34.80	–24:39:17.0	0.23	dahle+02	2002ApJS..139..313D	3.225	1.301	7.212	2.909	11.403	4.599	14.723	5.939
ZwCl 0104.4+0048	01:06:48.5	+01:02:42.0	0.2545	N	ZwCl 0104.4+0048	01:06:58.07	+01:04:01.4	0.2545	okabe+10	2010PASJ...62..811O	1.008	0.262	1.841	0.478	2.299	0.597	2.546	0.661
RX J0110.3+1938	01:10:18.22	+19:38:19.4	0.317	N	WARP J0110.3+1938	01:10:18.00	+19:38:23.0	0.317	hoekstra+11	2011ApJ...726...48H	0.580	0.300	1.585	0.820	2.363	1.222	2.796	1.446
ABELL 209	01:31:52.54	–13:36:40.4	0.206	N	ABELL 209	01:31:53.00	–13:36:34.0	0.206	umetsu+14	2014arXiv1404.1375U	4.033	0.688	11.573	1.796	17.559	2.993	21.473	3.922
ABELL 222	01:37:34.0	–12:59:29	0.213	N	ABELL 222	01:37:29.20	–12:59:10.0	0.213	mahdavi+13	2013ApJ...767..116M	1.572	0.555	5.649	1.246	8.559	1.888	10.417	2.298
ABELL 223S	01:37:56.0	–12:49:10	0.207	NA	NA NA	NA	NA	NA	mahdavi+13	2013ApJ...767..116M	1.003	0.482	6.863	1.936	10.435	2.943	12.738	3.593
ABELL 223N	01:38:02.3	–12:45:20	0.207	NA	NA NA	NA	NA	NA	hoekstra+12	2012MNRAS.427.1298H	2.100	0.550	5.500	1.900	8.320	2.142	10.100	2.600
RX J0142.0+2131	01:42:03.311	+21:31:22.64	0.28	N	MCXC J0142.0+2131	01:42:02.60	+21:31:19.0	0.2803	applegate+14	2014MNRAS.439...48A	1.847	0.743	4.621	1.860	6.678	2.688	7.858	3.162
CL J0152-1357	01:52:41.0	–13:57:45	0.84	N	WARP J0152.7-1357	01:52:41.00	–13:57:45.0	0.831	sereno&13	2013MNRAS.434..878S	1.382	0.291	2.259	0.475	2.800	0.589	2.964	0.624
ABELL 267	01:52:42.0	+01:00:26	0.23	N	ABELL 267	01:52:52.26	+01:02:45.8	0.231	mahdavi+13	2013ApJ...767..116M	2.053	0.428	5.245	1.523	7.948	2.308	9.637	2.798
RX J0154.2-5937	01:54:13.72	–59:37:31.0	0.36	N	400d J0154-5937	01:54:14.80	–59:37:48.0	0.36	hoekstra+11	2011ApJ...726...48H	0.340	0.200	0.910	0.535	1.348	0.793	1.578	0.928
CL 0159+0030	01:59:18.2	+00:30:09	0.39	N	NSCS J015924+003024	01:59:17.00	+00:30:10.4	0.386	israel+12	2012A%26A...546A..79I	1.443	0.634	3.466	1.524	4.937	2.170	5.671	2.493
CFHTLS c12-w1	02:01:18.00	–07:39:03.60	0.14	NA	NA NA	NA	NA	NA	shan+12	2012ApJ...748...56S	0.107	0.023	0.259	0.055	0.371	0.078	0.447	0.095
CFHTLS c3-w1	02:01:41.04	–05:01:48.00	0.28	NA	NA NA	NA	NA	NA	shan+12	2012ApJ...748...56S	0.987	0.183	2.813	0.522	4.257	0.790	5.104	0.947
ABELL 291	02:01:44.2	–02:12:03.0	0.196	N	ABELL 291	02:01:44.20	–02:12:03.0	0.197	okabe+10	2010PASJ...62..811O	1.166	0.345	5.222	1.545	9.022	2.669	11.658	3.448
CFHTLS c16-w1	02:01:48.48	–10:51:10.80	0.66	NA	NA NA	NA	NA	NA	shan+12	2012ApJ...748...56S	0.617	0.094	1.870	0.284	2.892	0.440	3.289	0.500
CFHTLS c14-w1	02:02:08.16	–08:26:13.20	0.4	P	GMBCG J030.53418-08.43703	02:02:08.20	–08:26:13.3	0.349	shan+12	2012ApJ...748...56S	0.458	0.054	1.285	0.151	1.934	0.227	2.262	0.266
CFHTLS c2-w1	02:02:30.00	–03:57:57.60	0.48	NA	NA NA	NA	NA	NA	shan+12	2012ApJ...748...56S	4.884	2.826	16.261	9.408	26.022	15.057	30.663	17.742
CFHTLS c13-w1	02:02:49.92	–09:20:13.20	0.23	P	ABELL 298	02:02:48.90	–09:19:57.0	0.14315	shan+12	2012ApJ...748...56S	0.054	0.031	0.130	0.075	0.185	0.107	0.219	0.126
CFHTLS c6-w1	02:03:21.60	–07:19:51.60	0.27	NA	NA NA	NA	NA	NA	shan+12	2012ApJ...748...56S	0.258	0.057	0.678	0.150	0.997	0.221	1.184	0.262
CFHTLS c5-w1	02:03:26.40	–05:55:30.00	0.38	NA	NA NA	NA	NA	NA	shan+12	2012ApJ...748...56S	0.246	0.052	0.662	0.139	0.981	0.206	1.146	0.241
CFHTLS c15-w1	02:03:28.80	–09:49:01.20	0.32	P	GMBCG J030.86962-09.81667	02:03:28.71	–09:49:00.0	0.33	shan+12	2012ApJ...748...56S	0.220	0.055	0.580	0.145	0.854	0.213	1.005	0.251
CFHTLS c9-w1	02:03:32.16	–06:44:09.60	0.81	NA	NA NA	NA	NA	NA	shan+12	2012ApJ...748...56S	1.042	0.261	3.371	0.845	5.339	1.338	6.012	1.507
CFHTLS c1-w1	02:03:57.60	–04:13:22.80	0.18	NA	NA NA	NA	NA	NA	shan+12	2012ApJ...748...56S	1.956	1.176	5.652	3.398	8.597	5.168	10.562	6.350
CFHTLS c7-w1	02:04:18.48	–07:12:46.80	0.33	NA	NA NA	NA	NA	NA	shan+12	2012ApJ...748...56S	0.682	0.486	1.924	1.372	2.903	2.070	3.442	2.455
CFHTLS c22-w1	02:05:05.28	–05:55:22.80	0.41	NA	NA NA	NA	NA	NA	shan+12	2012ApJ...748...56S	0.088	0.055	0.224	0.141	0.327	0.206	0.377	0.238
CFHTLS c26-w1	02:05:16.80	–07:40:48.00	0.24	NA	NA NA	NA	NA	NA	shan+12	2012ApJ...748...56S	0.169	0.056	0.431	0.142	0.627	0.207	0.745	0.246
CFHTLS c24-w1	02:05:25.92	–07:35:16.80	0.4	P	CFHTLS:[DAC2011] W1-0493	02:05:25.92	–07:35:22.6	0.47	shan+12	2012ApJ...748...56S	0.455	0.185	1.275	0.520	1.919	0.782	2.245	0.915
CFHTLS c27-w1	02:06:22.80	–08:48:25.20	0.26	NA	NA NA	NA	NA	NA	shan+12	2012ApJ...748...56S	0.653	0.414	1.807	1.146	2.706	1.716	3.244	2.057
CFHTLS c28-w1	02:07:04.56	–08:29:42.00	0.08	NA	NA NA	NA	NA	NA	shan+12	2012ApJ...748...56S	0.230	0.066	0.574	0.163	0.828	0.236	1.016	0.289
CFHTLS c18-w1	02:07:11.28	–04:00:07.20	0.25	NA	NA NA	NA	NA	NA	shan+12	2012ApJ...748...56S	2.256	1.374	6.711	4.087	10.313	6.282	12.523	7.628
CFHTLS c17-w1	02:08:05.04	–04:34:58.80	0.32	NA	NA NA	NA	NA	NA	shan+12	2012ApJ...748...56S	2.035	1.135	6.130	3.420	9.464	5.280	11.343	6.328
CFHTLS c39-w1	02:08:32.40	–07:43:48.00	0.34	NA	NA NA	NA	NA	NA	shan+12	2012ApJ...748...56S	0.817	0.528	2.337	1.511	3.543	2.291	4.200	2.716
CFHTLS c42-w1	02:09:15.12	–09:14:38.40	0.71	NA	NA NA	NA	NA	NA	shan+12	2012ApJ...748...56S	0.382	0.148	1.135	0.438	1.743	0.673	1.967	0.760
CFHTLS c33-w1	02:09:44.40	–05:43:48.00	0.23	NA	NA NA	NA	NA	NA	shan+12	2012ApJ...748...56S	0.340	0.038	0.899	0.101	1.325	0.150	1.588	0.179
ABELL 315	02:10:03.0	–00:59:52	0.1754	N	ABELL 315	02:10:03.06	–00:59:51.8	0.1754	dietrich+09	2009A%26A...499..669D	1.172	0.331	3.215	0.909	4.800	1.357	5.854	1.655

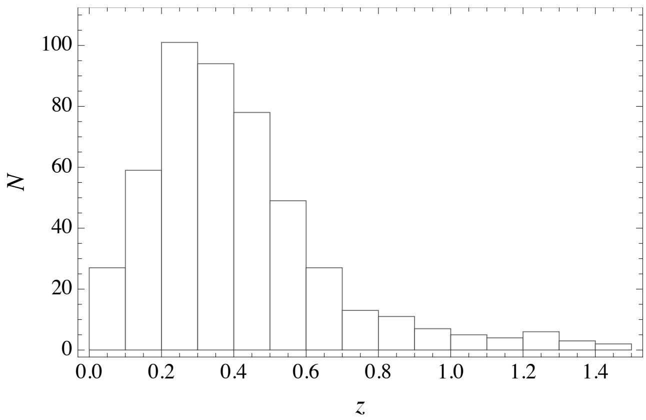

Figure 2. Redshift distribution of the 485 WL clusters in the LC^2-*single* catalog.

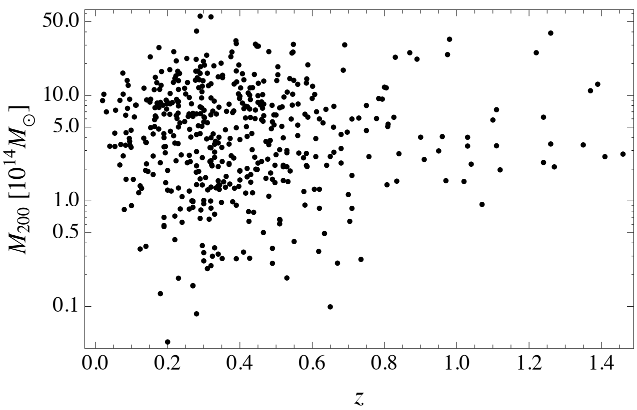

Figure 4. Redshift versus mass for the 485 WL clusters in the LC^2-*single* catalog. M_{200} is in units of $10^{14}M_\odot$.

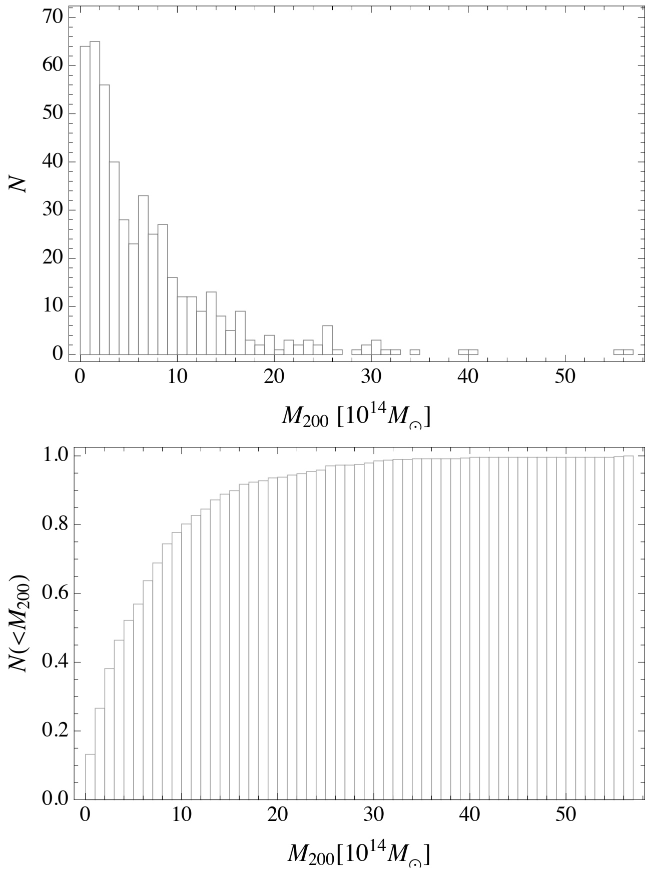

Figure 3. Mass distribution of the 485 WL clusters in the LC^2-*single* catalog. Top panel: binned histogram of the mass distribution; bottom panel: normalized cumulative function. M_{200} is in units of $10^{14}M_\odot$.

$0.02 \lesssim z \lesssim 1.46$, with a peak at $z \sim 0.35$, where lensing studies are optimised. The tail at large redshift includes 50 (20) clusters at $z > 0.7$ (1.0).

Weak lensing is better suited to measure massive clusters. The mass distribution has a median $M_{200} \sim 4.5 \times 10^{14} M_\odot$ and extends to M_{200} larger than $5 \times 10^{15} M_\odot$, see Fig. 3. Shear or X-ray selected groups of clusters mostly populate the less massive bins.

Due to the heterogeneous nature of the sample there is no evident trend in cluster masses with redshift, see Fig. 4. Approximated selection functions might be derived only for specific subsamples.

8 CONCLUSIONS

A standardised collection of weak lensing masses may be very useful for X-ray, SZ and other multi-wavelength studies. I compiled from literature three catalogues. The LC^2-*all*, -*single* and -*substructure* catalogs comprise 822, 485 and 18 groups and clusters, respectively.

The LC^2-*all* catalog is a repository of all the main information on clusters with measured lensing mass I found in literature. LC^2-*single* is a list of unique entries. LC^2-*substructure* focuses on complex structures.

The full catalogs are publicly available in electronic format[4]. The first version of the catalogs is released together with this presentation paper. The catalogs will be periodically updated.

ACKNOWLEDGEMENTS

I thank S. Ettori, L. Moscardini and K. Umetsu for fruitful discussions. I acknowledge financial contributions from contracts ASI/INAF I/023/12/0, by the PRIN MIUR 2010-2011 'The dark Universe and the cosmic evolution of baryons: from current surveys to Euclid' and by the PRIN INAF 2012 'The Universe in the box: multiscale simulations of cosmic structure'. I thank NASA. This research has made use of NASA's Astrophysics Data System (ADS) and of the NASA/IPAC Extragalactic Database (NED), which is operated by the Jet Propulsion Laboratory, California Institute of Technology, under contract with the National Aeronautics and Space Administration.

REFERENCES

Abate A., Wittman D., Margoniner V. E., Bridle S. L., Gee P., Tyson J. A., Dell'Antonio I. P., 2009, ApJ, 702, 603
Andreon S., Bergé J., 2012, A&A, 547, A117
Applegate D. E. et al., 2014, MNRAS, 439, 48

[4] www.dropbox.com/sh/hukhb24c3ahiun2/AADVuW7yUAA2XjyDrFwofejAa?dl=0

Arnaud M., Pratt G. W., Piffaretti R., Böhringer H., Croston J. H., Pointecouteau E., 2010, A&A, 517, A92
Bardeau S., Soucail G., Kneib J.-P., Czoske O., Ebeling H., Hudelot P., Smail I., Smith G. P., 2007, A&A, 470, 449
Becker M. R., Kravtsov A. V., 2011, ApJ, 740, 25
Biviano A. et al., 2013, A&A, 558, A1
Bradač M., Allen S. W., Treu T., Ebeling H., Massey R., Morris R. G., von der Linden A., Applegate D., 2008a, ApJ, 687, 959
Bradač M. et al., 2006, ApJ, 652, 937
Bradač M. et al., 2008b, ApJ, 681, 187
Bryan G. L., Norman M. L., 1998, ApJ, 495, 80
Clowe D., Gonzalez A., Markevitch M., 2004, ApJ, 604, 596
Clowe D., Luppino G. A., Kaiser N., Gioia I. M., 2000, ApJ, 539, 540
Clowe D. et al., 2006, A&A, 451, 395
Corless V. L., King L. J., Clowe D., 2009, MNRAS, 393, 1235
Cypriano E. S., Sodré, Jr. L., Kneib J.-P., Campusano L. E., 2004, ApJ, 613, 95
D'Agostini G., 2004, physics/0403086
Dahle H., 2006, ApJ, 653, 954
Dahle H., Kaiser N., Irgens R. J., Lilje P. B., Maddox S. J., 2002, ApJS, 139, 313
Diemer B., Kravtsov A. V., 2014, ArXiv: 1407.4730
Dietrich J. P., Biviano A., Popesso P., Zhang Y.-Y., Lombardi M., Böhringer H., 2009, A&A, 499, 669
Donahue M. et al., 2014, ArXiv: 1405.7876
Duffy A. R., Schaye J., Kay S. T., Dalla Vecchia C., 2008, MNRAS, 390, L64
Dutton A. A., Macciò A. V., 2014, MNRAS, 441, 3359
Ettori S., 2013, MNRAS, 435, 1265
Ettori S., Morandi A., Tozzi P., Balestra I., Borgani S., Rosati P., Lovisari L., Terenziani F., 2009, A&A, 501, 61
Foëx G., Soucail G., Pointecouteau E., Arnaud M., Limousin M., Pratt G. W., 2012, A&A, 546, A106
Gao L., Navarro J. F., Cole S., Frenk C. S., White S. D. M., Springel V., Jenkins A., Neto A. F., 2008, MNRAS, 387, 536
Gavazzi R., 2005, A&A, 443, 793
Gavazzi R., Adami C., Durret F., Cuillandre J.-C., Ilbert O., Mazure A., Pelló R., Ulmer M. P., 2009, A&A, 498, L33
Gavazzi R., Mellier Y., Fort B., Cuillandre J.-C., Dantel-Fort M., 2004, A&A, 422, 407
Gavazzi R., Soucail G., 2007, A&A, 462, 459
Giocoli C., Meneghetti M., Ettori S., Moscardini L., 2012, MNRAS, 426, 1558
Giocoli C., Meneghetti M., Metcalf R. B., Ettori S., Moscardini L., 2014, MNRAS, 440, 1899
Giodini S., Lovisari L., Pointecouteau E., Ettori S., Reiprich T. H., Hoekstra H., 2013, Space Science Reviews, 177, 247
Gott, III J. R., Vogeley M. S., Podariu S., Ratra B., 2001, ApJ, 549, 1
Gray M. E., Taylor A. N., Meisenheimer K., Dye S., Wolf C., Thommes E., 2002, ApJ, 568, 141
Gruen D. et al., 2014, MNRAS, 442, 1507
Halkola A., Seitz S., Pannella M., 2006, MNRAS, 372, 1425
Hamana T., Miyazaki S., Kashikawa N., Ellis R. S., Massey R. J., Refregier A., Taylor J. E., 2009, PASJ, 61, 833
Hamilton-Morris V., Smith G. P., Edge A. C., Egami E., Haines C. P., Marshall P. J., Sanderson A. J. R., Targett T. A., 2012, ApJ, 748, L23
Hicks A. K. et al., 2007, ApJ, 671, 1446
High F. W. et al., 2012, ApJ, 758, 68
Hoekstra H., Donahue M., Conselice C. J., McNamara B. R., Voit G. M., 2011, ApJ, 726, 48
Hoekstra H., Mahdavi A., Babul A., Bildfell C., 2012, MNRAS, 427, 1298
Hu W., Kravtsov A. V., 2003, ApJ, 584, 702
Huang Z., Radovich M., Grado A., Puddu E., Romano A., Limatola L., Fu L., 2011, A&A, 529, A93
Israel H., Erben T., Reiprich T. H., Vikhlinin A., Sarazin C. L., Schneider P., 2012, A&A, 546, A79
Jauzac M. et al., 2014, ArXiv: 1406.3011
Jauzac M. et al., 2012, MNRAS, 426, 3369
Jee M. J. et al., 2011, ApJ, 737, 59
Jee M. J., Hughes J. P., Menanteau F., Sifón C., Mandelbaum R., Barrientos L. F., Infante L., Ng K. Y., 2014, ApJ, 785, 20
Jee M. J., Tyson J. A., 2009, ApJ, 691, 1337
Jee M. J., White R. L., Benítez N., Ford H. C., Blakeslee J. P., Rosati P., Demarco R., Illingworth G. D., 2005a, ApJ, 618, 46
Jee M. J., White R. L., Ford H. C., Blakeslee J. P., Illingworth G. D., Coe D. A., Tran K.-V. H., 2005b, ApJ, 634, 813
Jee M. J., White R. L., Ford H. C., Illingworth G. D., Blakeslee J. P., Holden B., Mei S., 2006, ApJ, 642, 720
Jing Y. P., Suto Y., 2002, ApJ, 574, 538
Jullo E., Natarajan P., Kneib J.-P., D'Aloisio A., Limousin M., Richard J., Schimd C., 2010, Science, 329, 924
Kettula K. et al., 2013, ApJ, 778, 74
Kubo J. M. et al., 2009, ApJ, 702, L110
Kubo J. M., Stebbins A., Annis J., Dell'Antonio I. P., Lin H., Khiabanian H., Frieman J. A., 2007, ApJ, 671, 1466
LaRoque S. J., Bonamente M., Carlstrom J. E., Joy M. K., Nagai D., Reese E. D., Dawson K. S., 2006, ApJ, 652, 917
Laureijs R. et al., 2011, ArXiv: 1110.3193
Lemze D., Broadhurst T., Rephaeli Y., Barkana R., Umetsu K., 2009, ApJ, 701, 1336
Lerchster M. et al., 2011, MNRAS, 411, 2667
Limousin M. et al., 2009, A&A, 502, 445
Limousin M. et al., 2010, MNRAS, 405, 777
Limousin M., Morandi A., Sereno M., Meneghetti M., Ettori S., Bartelmann M., Verdugo T., 2013, Space Science Reviews, 177, 155
Limousin M. et al., 2007, ApJ, 668, 643
Lubini M., Sereno M., Coles J., Jetzer P., Saha P., 2013, MNRAS submitted
Mahdavi A., Hoekstra H., Babul A., Bildfell C., Jeltema T., Henry J. P., 2013, ApJ, 767, 116
Mahdavi A., Hoekstra H., Babul A., Sievers J., Myers S. T., Henry J. P., 2007, ApJ, 664, 162
Mantz A., Allen S. W., Rapetti D., Ebeling H., 2010, MNRAS, 406, 1759
Margoniner V. E., Lubin L. M., Wittman D. M., Squires G. K., 2005, AJ, 129, 20
McInnes R. N., Menanteau F., Heavens A. F., Hughes J. P., Jimenez R., Massey R., Simon P., Taylor A., 2009, MNRAS, 399, L84
Medezinski E., Broadhurst T., Umetsu K., Oguri M., Rephaeli Y., Benítez N., 2010, MNRAS, 405, 257
Melchior P. et al., 2014, ArXiv: 1405.4285
Menanteau F. et al., 2013, ApJ, 765, 67
Meneghetti M., Fedeli C., Zitrin A., Bartelmann M., Broadhurst T., Gottlöber S., Moscardini L., Yepes G., 2011, A&A, 530, A17
Meneghetti M., Rasia E., Merten J., Bellagamba F., Ettori S., Mazzotta P., Dolag K., Marri S., 2010, A&A, 514, A93
Merten J. et al., 2011, MNRAS, 417, 333
Merten J. et al., 2014, ArXiv: 1404.1376

Miyatake H. et al., 2013, MNRAS, 429, 3627
Morandi A. et al., 2012, MNRAS, 425, 2069
Navarro J. F., Frenk C. S., White S. D. M., 1996, ApJ, 462, 563
Neto A. F. et al., 2007, MNRAS, 381, 1450
Oguri M., Bayliss M. B., Dahle H., Sharon K., Gladders M. D., Natarajan P., Hennawi J. F., Koester B. P., 2012, MNRAS, 420, 3213
Oguri M., Blandford R. D., 2009, MNRAS, 392, 930
Oguri M. et al., 2013, MNRAS, 429, 482
Oguri M., Takada M., Umetsu K., Broadhurst T., 2005, ApJ, 632, 841
Okabe N., Bourdin H., Mazzotta P., Maurogordato S., 2011, ApJ, 741, 116
Okabe N., Futamase T., Kajisawa M., Kuroshima R., 2014a, ApJ, 784, 90
Okabe N., Smith G. P., Umetsu K., Takada M., Futamase T., 2013, arXiv:1302.2728
Okabe N., Takada M., Umetsu K., Futamase T., Smith G. P., 2010, PASJ, 62, 811
Okabe N., Umetsu K., 2008, PASJ, 60, 345
Okabe N. et al., 2014b, ArXiv: 1406.3451
Paulin-Henriksson S., Antonuccio-Delogu V., Haines C. P., Radovich M., Mercurio A., Becciani U., 2007, A&A, 467, 427
Pedersen K., Dahle H., 2007, ApJ, 667, 26
Piffaretti R., Arnaud M., Pratt G. W., Pointecouteau E., Melin J.-B., 2011, A&A, 534, A109
Planck Collaboration et al., 2013, ArXiv: 1303.5080
Prada F., Klypin A. A., Cuesta A. J., Betancort-Rijo J. E., Primack J., 2012, MNRAS, 423, 3018
Pratt G. W., Croston J. H., Arnaud M., Böhringer H., 2009, A&A, 498, 361
Radovich M., Puddu E., Romano A., Grado A., Getman F., 2008, A&A, 487, 55
Rasia E. et al., 2012, New Journal of Physics, 14, 055018
Reichardt C. L. et al., 2013, ApJ, 763, 127
Rines K., Diaferio A., 2006, AJ, 132, 1275
Romano A. et al., 2010, A&A, 514, A88
Rozo E., Rykoff E. S., Bartlett J. G., Evrard A., 2014, MNRAS, 438, 49
Schirmer M., Hildebrandt H., Kuijken K., Erben T., 2011, A&A, 532, A57
Schirmer M., Suyu S., Schrabback T., Hildebrandt H., Erben T., Halkola A., 2010, A&A, 514, A60
Sereno M., 2002, A&A, 393, 757
Sereno M., 2007, MNRAS, 380, 1207
Sereno M., Covone G., 2013, MNRAS, 434, 878
Sereno M., Ettori S., 2014, ArXiv: 1407.7868
Sereno M., Ettori S., Moscardini L., 2014, ArXiv: 1407.7869
Sereno M., Ettori S., Umetsu K., Baldi A., 2013, MNRAS, 428, 2241
Sereno M., Giocoli C., Ettori S., Moscardini L., 2014, in preparation
Sereno M., Jetzer P., Lubini M., 2010, MNRAS, 403, 2077
Sereno M., Umetsu K., 2011, MNRAS, 416, 3187
Sereno M., Zitrin A., 2012, MNRAS, 419, 3280
Shan H. et al., 2012, ApJ, 748, 56
Smail I., Ellis R. S., Dressler A., Couch W. J., Oemler A., Sharples R. M., Butcher H., 1997, ApJ, 479, 70
Tinker J., Kravtsov A. V., Klypin A., Abazajian K., Warren M., Yepes G., Gottlöber S., Holz D. E., 2008, ApJ, 688, 709
Umetsu K. et al., 2009, ApJ, 694, 1643
Umetsu K., Broadhurst T., Zitrin A., Medezinski E., Hsu L.-Y., 2011, ApJ, 729, 127
Umetsu K. et al., 2014, ArXiv: 1404.1375
Voit G. M., 2005, Reviews of Modern Physics, 77, 207
von der Linden A. et al., 2014, MNRAS, 439, 2
Watanabe E. et al., 2011, PASJ, 63, 357
Wold M., Lacy M., Dahle H., Lilje P. B., Ridgway S. E., 2002, MNRAS, 335, 1017
Wright C. O., Brainerd T. G., 2000, ApJ, 534, 34